Fractional locking of spin-torque oscillator by injected ac current

Dong Li,[1] Yan Zhou,[2] Changsong Zhou,[1,*] and Bambi Hu[3]

[1]*Department of Physics, Centre for Nonlinear Studies and The Beijing-Hong Kong-Singapore Joint Centre for Nonlinear and Complex Systems (Hong Kong), Hong Kong Baptist University, Kowloon Tong, Hong Kong*

[2]*Department of Information Technology, Hong Kong Institute of Technology, Mid-levels west, Hong Kong*

[3]*Department of Physics, University of Houston, Houston, Texas 77204-5005, USA*

(Received 4 January 2011; revised manuscript received 21 March 2011; published 11 May 2011)

Fractional synchronization is one of the most interesting collective behaviors in coupled or driving-response oscillators system, very important for both a deep understanding of a particular oscillator and for its applications. We numerically investigate the fractional synchronization of a spin-torque oscillator by injected ac current. Multiple $p:q$ locking regions are found, which display some sophisticated overlaps. The system can be analyzed as a perturbed heteroclinic cycle rather than a phase oscillator. Both the modulations on the output frequency and power are mainly due to the modulation by the external signals on the distance between the dynamical orbit and the saddle point in phase space. By using this dynamical picture, we can well understand all the numerical results, including the variation of the locking region with the amplitude $|J_a|$ or frequency f of the injected signal, the influence by noise, and the difference among the output powers of coexisting locking attractors. These understandings are significant for both potential applications in electronic communications and a deep investigation into this novel device.

DOI: 10.1103/PhysRevB.83.174424 PACS number(s): 75.40.Gb, 85.75.Bb, 05.45.Xt

I. INTRODUCTION

The spin-torque oscillator (STO)[1] currently is receiving a rapidly growing interest thanks to its significant advantages, such as its extremely small footprint (without the need of a large inductor), ultrawide-band-frequency operation, and easy on-chip integration, which make it very promising for broadband high-quality microwave generator.[2] It is of significance to study the interaction between a STO and an external stimuli both for a deep understanding of the dynamical characteristics of a STO device and for potential applications. For example, for the purpose of utilizing that STO in most of the existing communication technology, it is imperative that it be readily modulated by an external stimuli since a pure microwave resonance of the STO does not carry any information.[3] When the external frequency f is close to the intrinsic (free-evolving) STO frequency F, it is possible to get a $1:1$ phase locking, where the locking ratios $p:q = f:\tilde{F} = 1:1$, and $\tilde{F}$ is the oscillation frequency of the STO under external forces. This effect has been studied both experimentally and theoretically for the purpose of understanding and realization of mutual synchronization of two or more STOs.[4]

Understanding the response of a STO to a wider range of injected frequencies can be obtained by investigating the fractional synchronization, which means $p:q$ is a rational number. Urazhdin *et al.*[5] experimentally demonstrated that the STO can be fractionally locked to a microwave magnetic field and pointed out that the nontrivial observation was due to the complex nonlinear characteristics of STO. Microwave magnetic field and microwave current are the two external stimuli that are usually used to interact with STOs. However, it will be much more convenient to modulate the STO with an external microwave current instead of a microwave magnetic field since the incorporation of a large magnetic field source for the generation of a microwave field will outweigh any advantages of STO-based nanosized devices.[6] In this paper, we will study the fractional synchronization of the STO with a wide range of injected ac currents.[5]

Previously, such a driven STO has usually been analyzed by phase oscillator model, where the synchronization is usually associated with a $1:1$ locking when the driving frequency is close to the free-evolving frequency.[4,7] But the phase oscillator model cannot be used to explain some important nonlinear characteristics.[8] Therefore, it is not expected to be suitable to analyze most of the phenomena relating to $p:q$ fractional locking, since the appearance of $p:q$ locking usually is associated with some highly nonlinear characteristics. The STO is a nonlinear oscillatory system with some saddle-connection structures, and its dynamics is more suitably analyzed as a perturbed heteroclinic cycle.[8] In this type of dynamical system, there is a good degree of flexibility of locking in a wide range of both subharmonics and superharmonics, which comes from the sensitivity of its dynamical state near the heteroclinic orbit, especially near the saddle points.[9] This is the theoretical foundation basis on which we analyze the $p:q$ fractional locking of STO.

Three problems are of special importance in studying locking behavior. First, how do these $p:q$ locking regions change with the parameters of the driving signals? They can highly reflect the nonlinear characteristics of a particular system.[5,10] Second, how do these regions change if noise effect is taken into consideration? It is important because noise plays a unique role in such a dynamical system with a saddle-connection structures[9,11] and noise is inevitable in the experiments.[12] Third, what is the output power of these locking attractors? The output power is of importance for its applications.[2]

Our studies in this paper will be focused on the aforementioned three problems. Multiple $p:q$ locking regions are found, and their rich behaviors are shown. The STO system has a great degree of flexibility of locking to a wide range of injected frequencies than that of a typical driven phase

oscillator. Different $p:q$ fractional locking regions can have complicated overlaps, and multiple $p:q$ locking attractors can coexist at the same system parameters. Noise can destroy the attracting basins of the locking attractor having the smallest distance to its bifurcation point in parameter space or the one having the smallest attracting basin. Noise can also make the STO lock to a slower injected frequency. The output power is different among the coexisting locking attractors. These nontrivial features must be taken into consideration when developing STOs into applications. Importantly, all the observations can be well understood by the nonlinearity of the perturbed heteroclinic cycle structure, i.e., the results of the modulation on the frequency or on the output power indeed comes from the modulation on the distance between the dynamical orbit and the saddle point in the phase space, and the larger the distance, the slower the frequency. Through these detailed studies of fractional locking, the complex nonlinear characteristics of this nontrivial STO system can therefore be well understood.

II. MODEL

A macrospin approximation treats the magnetization of a sample as a single macroscopic spin and has been extensively used to capture some features of magnetic materials qualitatively as well as for studying the fundamental aspects of the spin-torque-induced magnetization precession and switching, albeit with some limitations, such as are typically used for studying nanopillar with lateral sizes below 30 nm where the dominant spin wave is a zero-order coherent spin wave mode; and it becomes invalid for the cases where the large-amplitude, higher-order spin wave modes excitations become important such as magnetic nanocontacts, vortex oscillators, and most of spin-torque-driven domain-wall motions. In this paper we utilize a macrospin approximation for studying the qualitative features of microwave-current-driven fractional locking of the mostly commonly investigated in-plane spin-torque nanopillar device injected with ac current [Fig. 1(a)]. The unit vector of the free-layer magnetization $\mathbf{m}$ is described by the Landau–Lifshitz–Gilbert–Slonczewski (LLGS) equation,[13]

$$\frac{d\mathbf{m}}{dt} = -|\gamma|\mathbf{m}\times\mathbf{H}_{\text{eff}} + \alpha\mathbf{m}\times\frac{d\mathbf{m}}{dt} + |\gamma|\beta J\mathbf{m}\times(\mathbf{m}\times\mathbf{M}), \tag{1}$$

where γ is the gyromagnetic ratio, α is the Gilbert damping parameter, and β contains material parameters and fundamental constants.[14] The electrical current J is defined as positive when electrons flow from the fixed layer to the free layer. The effective field $\mathbf{H}_{\text{eff}}$ carries the contribution of an external applied magnetic field H_a, an anisotropy (easy axis) field H_k along the x axis, and a demagnetization (easy plane anisotropy) field $\mu_0 H_{dz} = 4\pi M_s$, where M_s is the saturation magnetization of the free-layer material. Thus we get $\mathbf{H}_{\text{eff}} = H_a\hat{e}_x + (H_k m_x\hat{e}_x - H_{dz}m_z\hat{e}_z)/|\mathbf{m}|$. In most experiments, due to the utilization of a synthetic antiferromagnetic stucture such as a pinned layer, the stray field acting on the free layer can be significantly compensated. In the framework of macrospin simulation employed in the current study, the stray field acting on the free (sensing) layer is assumed to be zero.

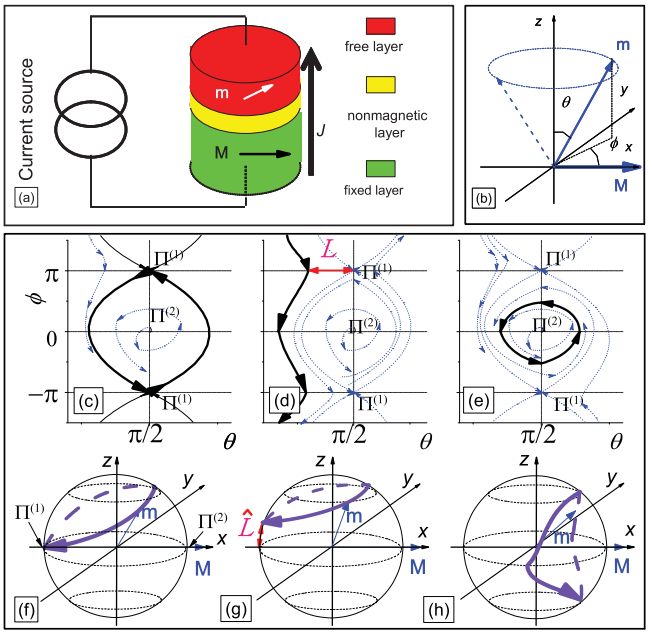

FIG. 1. (Color online) (a) Schematic of the in-plane STO investigated in this paper. The free-layer magnetization $\mathbf{m}$ is separated from the fixed layer $\mathbf{M}$ by a nonmagnetic layer. In the spherical coordinate system (b), the three possible oscillatory states in a free-evolving STO are shown respectively in (c) a attracting heteroclinic cycle, (d) global oscillation, and (e) local oscillation. The bold lines are the attractors. Their trajectories in the three-dimensional configuration space are shown respectively in (f) a homoclinic orbit, (g) out-of-plane oscillation, and (h) in-plane oscillation. L in (d) indicates the distance between the orbit and saddle. $\hat{L}$ in (g) demonstrate this distance in the configuration space.

In spherical coordinate system, we can express Eq. (1) as

$$\frac{d\theta}{dt} = \frac{\gamma}{1+\alpha^2}\{U\cos\theta\cos\phi + \alpha(H_{dz} + H_k\cos^2\phi) \times \sin\theta\cos\theta - V\sin\phi - H_k\sin\phi\cos\phi\sin\theta\}, \tag{2}$$

$$\frac{d\phi}{dt} = \frac{\gamma}{1+\alpha^2}\left\{\frac{1}{\sin\theta}[-U\sin\phi - (H_{dz} + H_k\cos^2\phi)\sin\theta \times\cos\theta - V\cos\phi\cos\theta - \alpha H_k\sin\phi\cos\phi\sin\theta]\right\}, \tag{3}$$

where $U = \alpha H_a - \beta(J_d + J_a)$ and $V = H_a + \alpha\beta(J_d + J_a)$. J_d is the dc current and $J_a = |J_a|\cos 2\pi f t$ represents the injected ac current with the amplitude $|J_a|$ and the injected frequency f. The values of some parameters used in the calculation are as follows: $|\gamma| = 1.885\times10^{11}$Hz/T, $\alpha = 10^{-2}$, $H_a = 0.2$ T, $\beta = 10/3$, $H_{dz} = 1.6$ T, $H_k = 0.05$ T, and $J_d = 10$ mA, so that the free-evolving frequency F approximates to 21.7 GHz.

We call it a free-evolving state when $|J_a| = 0$. In the parameter region where the STO can itself sustain an oscillation, the equilibrium state $\Pi^{(1)}$ that $\mathbf{m}$ is antiparallel to $\mathbf{M}$ must be a saddle point in the dynamical phase space, whereas the other equilibrium state $\Pi^{(2)}$ that $\mathbf{m}$ is parallel to $\mathbf{M}$ must be an unstable focus. There may be a homoclinic orbit (a heteroclinic cycle in spherical coordinate system) connecting the saddle, but it can just happen at a particular subset with zero measure in the parameter space. The heteroclinic cycle in spherical

coordinate [Fig. 1(b)] is shown in Fig. 1(c), and its trajectory in the three-dimensional configuration space is shown in Fig. 1(f). The dynamics of the system with parameters deviating from that for the heteroclinic cycle can be dealt with as a *perturbed heteroclinic cycle*. The asymptotic stable states can be classified into two cases: (i) global oscillation [Figs. 1(d) and 1(g)] which means the free layer **m** rotates around the current J, and (ii) local oscillation (LO) [Figs. 1(e) and 1(h)] which means **m** just vibrates near a particular direction.[8] Such three types of oscillation have also been numerically and/or analytically given in others' work.[15] In this paper, we will focus on the physically more relevant global oscillatory state except for special notes. Such a state has a free-evolving frequency F depending on the distance L between the orbit and the saddle point,[8] as shown in Fig. 1(d). While the free-evolving state studied in this paper is always a global oscillatory state, the orbit could be driven across the saddle point and becomes a local oscillatory one when the injected current is large.

III. FRACTIONAL SYNCHRONIZATION

In the presence of an injected current, the system is driven to a new orbit with a different distance $\tilde{L}$ from the saddle, and the frequency is modulated to $\tilde{F}$ mainly due to $\tilde{L}$. When the injected ac current J_a is small, it influences the system as another perturbation. The case of small J_a has been studied in Ref. 8, showing that the $1:1$ locking region is proportional to the injected $|J_a|$. Here, we consider a wider range of driving frequencies and stronger currents; the synchronization regions are shown in Fig. 2. In the case of a wider range of driving frequencies, several fractional locking regions could be observed even when $|J_a|$ is small. For example, in Fig. 2 (below the dashed line), the regions of locking ratios $p:q = 1:2$, $1:1$, $2:1$, and $3:1$ are obvious and well separated. In the following, we investigate these fractional locking regions and focus on the three aforementioned problems.

A. $p:q$ locking regions

Before investigating how the $p:q$ locking regions change with system parameters, we show that it is relatively easier to fractionally lock this system and get larger locking regions than typical driven phase oscillators. The reason is that the dynamical orbit in this type of system is very sensitive to external perturbation near the saddle points and easier to be driven to the target orbit of the synchronized frequency.[9] Typically, an oscillator which could be fractionally locked to a driving signal, when simplified to the form of phase oscillator, would take the following form:

$$d\phi/dt = 2\pi F + \mu \sum_{p,q} g_{p,q} \sin(2\pi q f t - p\phi), \qquad (4)$$

where F and f are the free-evolving and driving frequencies, respectively, μ is the driving strength, and $g_{p,q}$ is the weight of the $p:q$ driving component. Usually, $g_{p,q}$ is bigger with smaller p and q, so that the smaller p and q locking attractor is more stable and its locking region is usually larger.

When the other $p:q$ components could be ignored compared with $1:1$, this phase oscillator could be simplified as

$$d\phi/dt = 2\pi F + \mu \sin(2\pi f t - \phi), \qquad (5)$$

whose locking region is

$$2\pi|F - f| \leqslant \mu. \qquad (6)$$

If we regard the driven STO as a phase oscillator, the $1:1$ driving strength has the same order as $\frac{\beta\gamma}{1+\alpha^2}|J_a|$.[8,16] The $1:1$ locking region given by Eq. (6) (dashed line in Fig. 3, lower panel) is much smaller than the $1:1$ locking region in Fig. 2 at the same injected amplitude $|J_a|$.

Here, our aim is to show a simple comparison, so we preserve three terms of $p:q = 1:1$, $2:1$, and $3:1$ and assume that $g_{1,1} = g_{2,1} = g_{3,1} = 1$ (in physical case, usually $g_{1,1} > g_{2,1} > g_{3,1}$). μ is still assigned the value as $\frac{\beta\gamma}{1+\alpha^2}|J_a|$. In Fig. 3, we show the locking region of this simplified driven phase oscillator:

$$d\phi/dt = 2\pi F + \mu[\sin(2\pi f t - \phi) + \sin(2\pi f t - 2\phi) + \sin(2\pi f t - 3\phi)]. \qquad (7)$$

Two significant differences are observed between the real driven STO system (Fig. 2) and the driven phase oscillator system (Fig. 3). First, this driven STO system shows a much larger locking region of each fractional locking attractor, when comparing Fig. 2 with the lower panel of Fig. 3, both having the same scale of $|J_a|$. To get a similar size of locking region in the driven phase oscillators, the driving current $|J_a|$ needs to be enlarged by 2–3 orders of magnitude, as seen in upper panel of Fig. 3. Second, there could be many $p:q$ locking regions in the real STO system whereas the number of fractional locking regions in the driven phase oscillator depends on

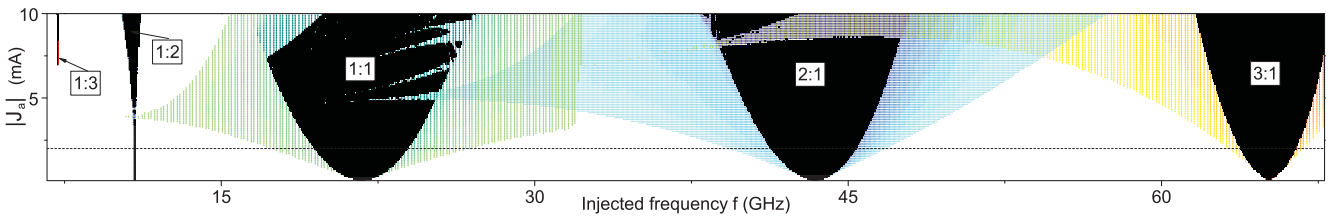

FIG. 2. (Color online) Probabilities of synchronization from different initial conditions in $1:3$, $1:2$, $1:1$, $2:1$, and $3:1$ regions. Black indicates the 100% synchronization regions. We use different color scales to help distinguish different locking regions. In each region, strips of the lighter color indicate smaller synchronization probabilities. Some other locking regions, such as $3:2$, $4:3$, etc., are also observed, but not shown in the figure for the sake of clarity). $|J_a| = 2$ mA is on the dashed line. The *probability* in this figure and also other places in this paper represents the ratio of the phase volume of an attracting basin to the whole phase space.

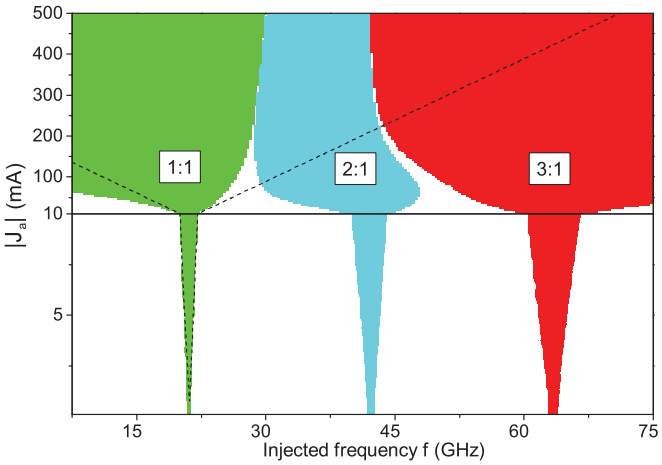

FIG. 3. (Color online) Fractional locking regions of the phase oscillator in Eq. (7). The lower panel has the same scale of $|J_a|$ as that of Fig. 2, but the locking regions are much smaller. To get a similar size of locking region to Fig. 2, the injected current $|J_a|$ needs to be enlarged greatly, as shown in the upper panel. The dashed lines delimit the 1 : 1 locking region of the driven phase oscillator, $d\phi/dt = 2\pi F + \beta|J_a|\sin(2\pi f t - \phi)$.

the form of the coupling term [in the case of Eq. (5), only 1 : 1 is found; in the case of Eq. (7), 2 : 1 and 3 : 1 locking emerge]. This comparison shows that the degree of flexibility of fractional synchronization of the driven STO system is quite high, consistent with the expectation based on the perturbed heteroclinic cycle structure. Several typical representations of the locking dynamics of the driven STO system are shown in Fig. 4.

In a typical oscillator which can be well described by a phase oscillator, increasing J_a of the driving signal will generally enlarge the locking region and make an locking attractor more stable, which can be beneficial for many

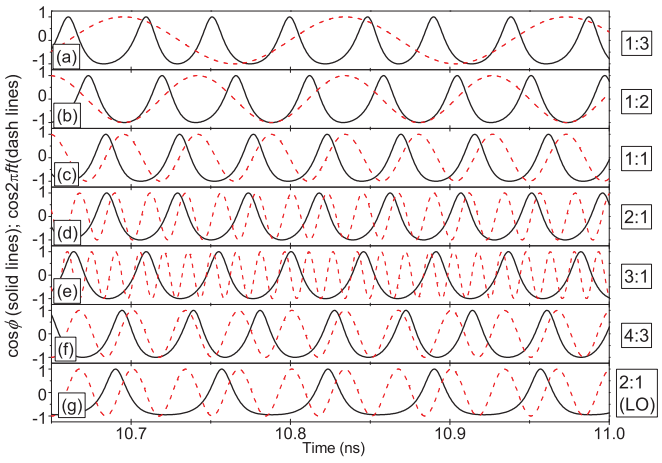

FIG. 4. (Color online) Time evolution of $\cos\phi$ (solid lines) and the injected signal $\cos(2\pi f t)$ (dashed lines) of several typical locking examples: (a) 1 : 3 ($f = 7.2$ GHz), (b) 1 : 2 ($f = 10.8$ GHz), (c) 1 : 1 ($f = 21.6$ GHz), (d) 2 : 1 ($f = 45.0$ GHz), (e) 3 : 1 ($f = 66.0$ GHz), (f) 4 : 3 ($f = 30.0$ GHz), and (g) 2 : 1 local oscillation ($f = 30.0$ GHz). $|J_a| = 10$ mA, and other parameters are the same as in Fig. 2. LO stands for local oscillation.

applications. However, this is not always the case in the driven STO system.

Comparing Fig. 2 and Fig. 3, we can see that when different $p : q$ locking regions meet, they may have some complicated overlaps. It is totally different from the $p : q$ locking in the driven phase oscillator, where the fractional locking regions are separated by obvious boundaries. This difference has significant implications in applications, because the overlapping of locking regions means that the attractor may not become more stable but rather could shift to another under some particular initial conditions when $|J_a|$ is increased. Here, multiple $p : q$ locking attractors can coexist for the same set of system parameters, for example the coexistence of 4 : 3 locking attractor and 2 : 1 locking attractor with [2 : 1(LO)], shown in Figs. 4(f) and 4(g). The problem happens when an expected 100% synchronization region is pierced by the locking regions of other attractors. For example, in the envelope of the 100% synchronization region of 1 : 1 locking in Fig. 2, synchronization may be expected to be achieved from any initial conditions, and then this synchronization region could be robustly employed in applications. However, this region is in fact pierced by other regions, e.g., 2 : 1, 3 : 1 locking, so the 1 : 1 synchronization is not always achievable. An example is shown in Fig. 5. When $f = 24.2$ GHz and $|J_a| = 3$ mA, 1 : 1 locking will be always achieved from any initial condition because it is the only attractor. But when increasing to $|J_a| = 5$ mA, the synchronization is invaded by 2 : 1 locking. From some particular initial conditions, 2 : 1 locking is achieved. When $|J_a|$ becomes larger, the overlaps of the coexisting multiple locking attractors and even some newly emergent ones will make the asymptotical dynamics depend strongly on initial conditions.

The sophisticated overlapping of different locking regions is a result of the saddle-node bifurcation of synchronization in the perturbed heteroclinic cycle system.[16] When a new locking attractor emerges, an unstable orbit emerges at the same parameter point, becoming the boundary of the attracting basin. So there is no need for the other attractors to lose

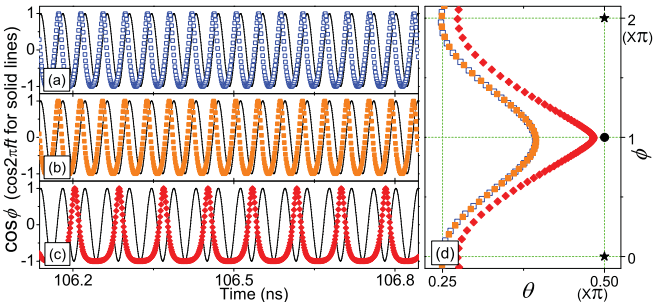

FIG. 5. (Color online) Time series of $\cos\phi$ of different locking attractors with the identical injected frequency $f = 24.2$ GHz. (a) 1 : 1 locking when $|J_a| = 3$ mA (unfilled squares), (b) 1 : 1 locking when $|J_a| = 5$ mA (filled squares), and (c) 2 : 1 locking when $|J_a| = 5$ mA (diamonds) compared with the driving signal $\cos 2\pi f t$ (solid line). (d) The dynamical orbits of these three attractors in phase space $\{\theta, \phi\}$. The filled circles and stars are respectively the saddle point $\Pi^{(1)}$ and unstable focus $\Pi^{(2)}$. The slower locking attractor (diamonds) shows an obviously shorter distance from the saddle point.

stability at the same time and multiple attractors can coexist as the overlap of the locking regions. On the other hand, a driven phase oscillator model in Eq. (4) is not relevant to explain this phenomenon, because the synchronization and desynchronization in phase oscillators are usually associated with supercritical Hopf bifurcation. When the synchronization attractor becomes stable, the other attractors must disappear, so that there are clear boundaries between locking regions.

According to our calculations within the framework of the perturbed heteroclinic cycle structure, the STO can demonstrate fractional locking to an ac current, which is similar to its fractional locking to an ac magnetic field, observed in experiments.[5] However, compared with the fractional locking by an ac field,[5] our studies show that the STO will exhibit different locking characteristics by an ac current, e.g., the overlapping of the locking regions, which has not been reported in the experiments by the ac magnetic field. Another difference refers to the size of the synchronization regions. As shown in Fig. 2, 1 : 1, 2 : 1, and 3 : 1 have similar synchronization regimes, different from the case of the ac field $p : 1$ phase locking, where the sizes of the synchronization regions are significantly different for even and odd p.

It should also be noticed that we simulate the *probability* in Fig. 2 and elsewhere by using uniform distribution of the initial conditions, so that the exact meaning of *probability* in fact reflects the ratio of the phase volume of an attracting basin to the whole phase space. The probabilities of these attractors in experiments is equivalent to the *probabilities* in this work with a weighting factor, which originates from the initial conditions' distribution affected by a variety of stochastic factors in reality, including, but not limited to, the temperature.

B. Noise effect

What the effect of noise is on these $p : q$ locking phenomena of the STO is another important problem. The great degree of flexibility of STO locking to a wide range is due to its sensitivity to the perturbation near saddle points.[9] Noise thus usually plays an important role in such a system.[11] And noise is inevitable in experiments. In the driven STO system, the influence of noise is more complex and interesting. It can influence both the locking frequency and the attracting basins of the coexisting locking attractors.

Let us first study the impact of noise on the locking frequency. Usually noise tends to drive the orbit far away from the saddle points in a pure heteroclinic cycle system, so as to speed up the oscillations.[11] Therefore it is often expected that the system tends to lock with a higher driving frequency when noise strength is increased. But in this system, there is already a perturbation induced by the system parameters, which makes the system have a higher opportunity of being driven close to the saddle in the presence of noise. As a result, the STO can be locked to a smaller driving frequency with some noise. But this phenomenon of noise-induced slowing down is not easily observed in a 1 : 1 locking region, because this locking region is usually too wide where the variation induced by noise is easily ignored. Thanks to the fractional synchronization states, we can demonstrate this nontrivial phenomenon obviously in a thinner locking region. As shown in the 1 : 2 region in Fig. 6(a), increasing Gaussian white noise can make the STO obviously lock to a smaller driving

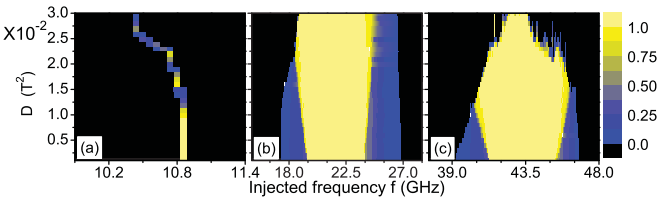

FIG. 6. (Color online) Probabilities of synchronization of (a) 1 : 2, (b) 1 : 1, and (c) 2 : 1 regions while noise added as $\langle H_a(t)\rangle = 0.2\text{T}$, $\langle H_a(t)H_a(s)\rangle = 2D\delta(t-s)$. $|J_a| = 2\text{mA}$ and the other parameters are the same as in Fig. 2.

frequency. The variation of locking frequency induced by noise is a typical phenomenon of synchronization in such a dynamical system with a saddle-connected structure, but the slowing-down phenomenon induced by noise is nontrivial. In these systems, the modulation by noise on the distance between the dynamical orbit and the saddle point results in a modulation on the frequency, one of the mechanisms underlying another well-known phenomenon named stochastic resonance.[17] In this way, noise can sometimes contribute to the locking of a STO to a different frequency. This effect is especially obvious when the locking region is small [comparing Fig. 6(a) with Figs. 6(b) and 6(c)]. It is therefore very important to consider the effect of noise in potential applications of STOs, especially in the case where the locked or modulated frequency is used to encode information.

The effect of noise on attracting basins is easier to comprehend. In the region of coexistence of multiple attractors, noise tends to destroy the basin of the locking attractor that has the smallest distance to its bifurcation point in parameter space, or the one with the smallest attracting basin. We demonstrate the meanings of the *smallest distance to its bifurcation point* and *smallest attracting basin* schematically in Fig. 7, where *initial conditions* refer to all the state variables, and ω could be any system parameter, e.g., the injected frequency f in our STO system. Along with the increasing ω, one can see the emergence of D and A and the disappearance of B, A, and C in order. At ω_1 and ω_2, A and B have the smallest distance to their bifurcation points S_1 and S_2, respectively. D has the smallest attracting basin at most region of the parameter ω.

In the driven STO system, by increasing the driving frequency f, different $p : q$ locking attractors can emerge and disappear in a way similar to that of Fig. 7. We show one of such examples in Fig. 8. Figures 8(a) and 8(b) respectively show the probabilities of getting each locking attractor with the uniform distribution of initial conditions in the absence and in the presence of noise, when the amplitude of the driving signal is fixed as $|J_a| = 10$ mA; Figs. 8(c), 8(e), 8(g), and 8(h) show the distributions of those attracting basins at $f = 29.1$ GHz, $f = 30.0$ GHz, $f = 30.3$ GHz, and $f = 15.9$ GHz; and Figs. 8(d) and 8(f) show two realizations of simulation in the presence of noise at $f = 29.1$ GHz and $f = 30.0$ GHz to demonstrate the change of the distributions of attracting basins and the smearing of the basins' boundaries.

Noise is absent at first. When f falls within the region between about 29.1 GHz and 30.0 GHz (1.38–1.43 times of F), the coexistent locking attractors are 1 : 1, 4 : 3, 3 : 2, and 2 : 1(LO) [Fig. 8(a)]. Similar to other fractional locking problems, the locking attractors with small p and q usually

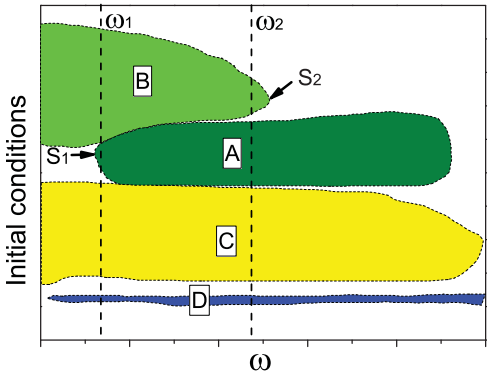

FIG. 7. (Color online) Schematic drawing of the bifurcation process versus ω in a dynamical system with the coexistence of multiple attractors, where ω could be any system parameter, e.g. the injected frequency f in our STO system. A, B, C, and D indicate the attracting basins of four $p:q$ locking attractors. S_1 indicates the bifurcation point of the emergence of A; S_2 indicates the bifurcation point of the disappearance of B. At ω_1 and ω_2, A and B have the smallest distance to their bifurcation point, respectively. D has the smallest attracting basin in most regions of the parameter ω.

exist in a wider region of system parameters, and they are usually more stable (having large basins),[10] e.g., C in Fig. 7 and the 1 : 1 locking in Fig. 8. When f increases to 30.3 GHz, the desynchronization attractor appears [Fig. 8(g)]. The output frequency of the 1 : 1 locking has the largest difference from the free-evolving frequency F. However, the 1 : 1 locking still has a longer distance to its bifurcation point of disappearance than 4 : 3 locking. The attracting basin of the desynchronization attractor does not invade the basin of the 1 : 1, but the basin of 4 : 3. With further increasing of f, 4 : 3 locking will disappear completely at about 30.6 GHz. The similar invasion happens to 3 : 2 locking when f decreases below 28.8 GHz. These observations show clearly that 1 : 1 locking appears to be more stable, whereas 4 : 3 is least stable at $f = 30.0$ GHz and 3 : 2 is least stable at $f = 29.1$ GHz.

The next question is, when noise is taken into consideration, which basin will be invaded first? The answer is that noise tends to invade the basin of 4 : 3 at $f = 30.0$ GHz or the basin of 3 : 2 at $f = 29.1$ GHz. It always invades the one having the smallest distance to its bifurcation point, because the existence of an attractor is sensitive to external perturbation when the system parameters are so close to the bifurcation point. Therefore the probabilities of achieving 4 : 3 locking at $f = 30.0$ GHz or 3 : 2 at $f = 29.1$ GHz significantly decrease, as shown in Fig. 8(b). We show a realization of simulation at $f = 29.1$ GHz with noise in Fig. 8(d), where the basin of 3 : 2 locking disappears completely due to noise. A similar phenomenon happens to the 4 : 3 locking at $f = 30.0$ GHz, shown in Fig. 8(f).

In other ranges of system parameters, the coexistent attractors are different; for example, we show in Fig. 8(h) that, at $f = 15.9$ GHz, the coexistent attractors turn out to be 1 : 1, 1 : 1(LO) and desynchronization state (DS), but the change of probabilities under noise effect is always similar.

Noise also tends to destroy the smallest attracting basin. In Fig. 7, D has the smallest basin and so does the 2 : 1 locking attractor of local oscillation in Fig. 8(a). Comparing Fig. 8(f) with Fig. 8(e), one can easily see that 2 : 1(LO) is no longer present under the noise effect. This change can also be observed by comparing Fig. 8(b) with Fig. 8(a). In Fig. 8(b), the probability of 2 : 1(LO) is zero, whereas in Fig. 8(a), it is not zero. But this comparison is not clear enough since the probability of 2 : 1(LO) is quite tiny in Fig. 8(a).

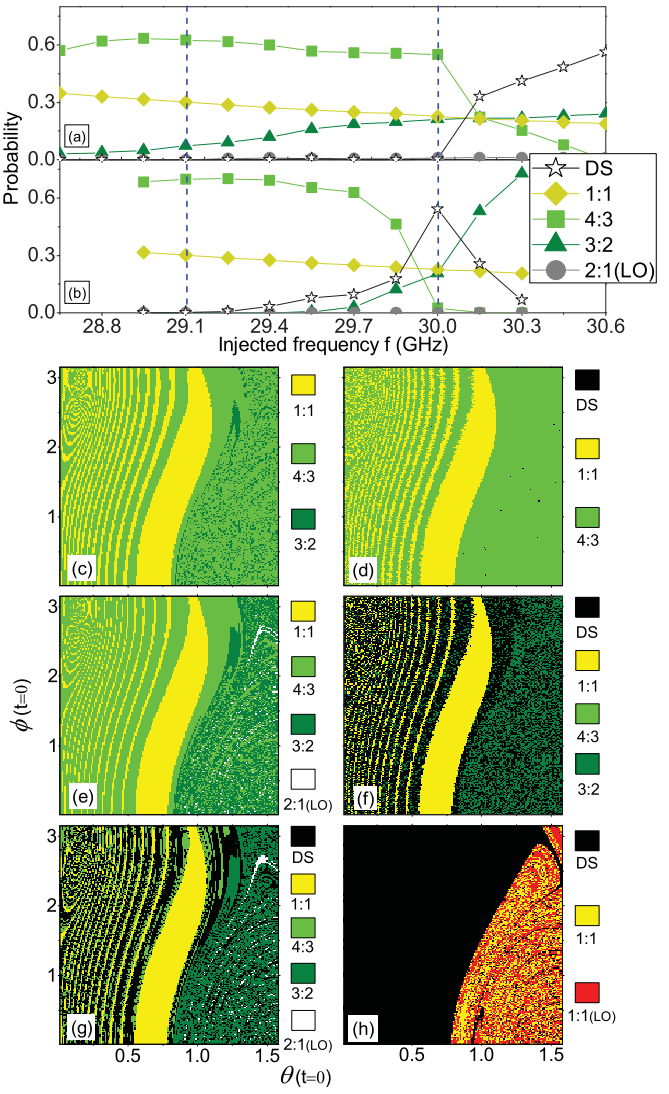

FIG. 8. (Color online) Attracting basins for the coexisting multiple attractors when $|J_a| = 10$ mA. (a) In the absence of noise, when f is between about 29.1 GHz and 30.0 GHz (the vertical dashed lines), locking attractors of 1 : 1, 4 : 3, 3 : 2 obviously coexist. [2 : 1 (LO) also exists, but its probability is too small.] (b) In the presence of noise of $\langle H_a(t)\rangle = 0.2$ T, $\langle H_a(t)H_a(s)\rangle = 0.01\delta(t-s)\mathrm{T}^2$, the probabilities of these attractors significantly change: the 3 : 2's turn out to be negligible at about $f = 29.1$ GHz, the 4 : 3's turn out to be negligible at about $f = 30.0$ GHz, and the 2 : 1(LO)s completely disappear for the whole region. (c) The distribution of attracting basins at $f = 29.1$ GHz, and (d) one of its realizations of simulation in the presence of noise demonstrates the change of the distribution and the smearing of the basins' boundaries. (e) The attracting basins at $f = 30.0$ GHz and (f) one of their realizations in the presence of noise. (g) The attracting basins at $f = 30.3$ GHz. (h) An example of the distribution of attracting basins far from the aforementioned parameter region, while $f = 15.9$ GHz. DS stands for the desynchronization state.

Now let us get back to discussing Figs. 6(b) and 6(c). Note that 100% synchronization state is most significante in applications because it is independent of initial conditions. An interesting question is whether noise can contribute to increasing the 100% synchronization state if the basins of other attractors are very small. The answer is yes. In Fig. 6(b) and Fig. 6(c), it is seen that, when the probability of synchronization is quite close to 100%, increasing noise can enhance it to 100% and make the 100% region wider and wider until noise strength is too large and it destroys synchronization again. On the other hand, when probabilities of synchronization are low, noise will always destroy the synchronization state.

These effects of noise on the attracting basins resulted from the particular bifurcation process as demonstrated in Fig. 7. The saddle-node bifurcation of synchronization in this perturbed heteroclinic cycle system is therefore crucial. All the nontrivial effects of noise originate from the role of noise to modulate the dynamical orbits near the saddle points in phase space in such a system with a perturbed heteroclinic cycle structure. Thus, a driven phase oscillator model is not relevant to explain these effects.

C. Output power

Besides all aforementioned dynamical behaviors, the output power is another important issue, since it is tied to applications of the system. The emitted microwave power spectra of the STO depends on a wide range of material parameters. Here we study how the output power is influenced by external driving signals. We have performed the Fourier transformations of $\sin\theta\cos\phi$, the cosine function of the relative angle between **m** and **M**, which is proportional with the STO output signal, to reflect the microwave power. The perturbed heteroclinic cycle structure can help us easily know the difference among the output powers of the coexisting locking attractors. The faster attractor oscillates farther away from the saddle point, usually with a smaller amplitude of oscillation,[8] leading to a smaller output power. Figure 9(a) shows the simulation results. The dashed line demonstrates the comparison we analyzed (which can be simply marked as $3:2 > 4:3 > 1:1$). The positions of these attractors in phase space $\{\theta,\phi\}$ are shown in Fig. 9(b). When $q \neq 1$, the distances between an orbit and the saddle point $\Pi^{(1)}$ have a little difference each time it gets close to the saddle point $\Pi^{(1)}$ since one $p:q$ attractor gets back to its original position after it passes over the saddle point for q times (rotates q cycles in configuration space). However, one can still easily notice the significant difference among the distances between each orbit and the saddle points. The significant difference among the distances induces different locking frequencies, and oscillatory amplitudes, leading to different output power.

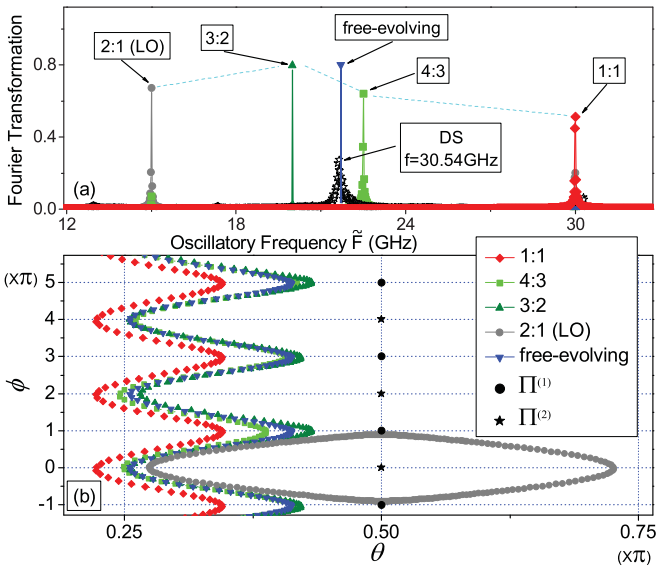

FIG. 9. (Color online) (a) Fourier transformation amplitudes of the cosine function of the relative angle between **m** and **M** of different attractors and (b) the positions of their orbits in phase space $\{\theta,\phi\}$. Parameters are the same as in Fig. 8(e), except for that in the free-evolving state $|J_a| = 0$ and in the desynchronization state $f = 30.3$ GHz. The dashed lines in (a) demonstrate the comparison among the output powers of the coexisting synchronization state.

IV. DISCUSSION

To gain a deeper understanding of how the STO device responses to a wide range of injected frequencies, we study the fractional synchronization of STO by an injected ac current. Multiple $p:q$ locking regions are observed. Our studies focus on three important problems: how do the locking regions change with driving parameters, how does noise affect the $p:q$ locking phenomenon, and what is the output power of these $p:q$ locking attractors? First, we found that the system has a great degree of flexibility of locking to a wide range of driving frequencies. The locking regions can have some sophisticated overlaps, where multiple $p:q$ attractors can coexist at the same system parameters. Even some 100% synchronization regions can be merged by other locking regions. Second, noise plays a nontrivial role. It can make the STO lock to relatively slower frequencies, and it can also destroy the attracting basin of the locking attractor having the smallest distance to its bifurcation point, or the one having the smallest attracting basin. Finally, we showed that the output power of the coexistent locking attractors depends on the oscillating frequencies.

All these novel dynamical behaviors were well explained by the perturbed heteroclinic cycle structures. Our studies are significant both for understanding the nonlinear characteristics of the STO system and for potential applications.

Our work can also help understand better about the dynamical behavior of the LLGS equation and thus shed light on a broad range of magnetism problems which can be described by this equation.[18]

ACKNOWLEDGMENTS

This work is support by Hong Kong Baptist University and conducted using the resources of the High Performance Cluster Computing Centre, Hong Kong Baptist University, which receives funding from Research Grant Council, University Grant Committee of the HKSAR, and Hong Kong Baptist University.

*cszhou@hkbu.edu.hk

[1]J. A. Katine, F. J. Albert, R. A. Buhrman, E. B. Myers, and D. C. Ralph, Phys. Rev. Lett. **84**, 3149 (2000); D. Houssameddine, U. Ebels, B. Delaet, B. Rodmacq, I. Firastrau, F. Ponthenier, M. Brunet, C. Thirion, J.-P. Michel, L. Prejbeanu-Buda, M.-C. Cyrille, O. Redon, and B. Dieny, Nat. Mater. **6**, 447 (2007); J. Katine and E. Fullerton, J. Magn. Magn. Mater. **320**, 1217 (2008); D. Ralph and M. Stiles, *ibid.* **321**, 2508 (2009); Y. Zhou and J. Akerman, Appl. Phys. Lett. **94**, 112503 (2009).

[2]M. Pufall, W. Rippard, S. Kaka, T. Silva, and S. Russek, Appl. Phys. Lett. **86**, 082506 (2005); T. J. Silva and W. H. Rippard, J. Magn. Magn. Mater. **320**, 1260 (2008).

[3]M. R. Pufall, W. H. Rippard, S. Kaka, T. J. Silva, and S. E. Russek, Appl. Phys. Lett. **86**, 082506 (2005).

[4]W. H. Rippard, M. R. Pufall, S. Kaka, T. J. Silva, S. E. Russek, and J. A. Katine, Phys. Rev. Lett. **95**, 067203 (2005); B. Georges, J. Grollier, M. Darques, V. Cros, C. Deranlot, B. Marcilhac, G. Faini, and A. Fert, *ibid.* **101**, 017201 (2008); Y. Zhou, J. Persson, S. Bonetti, and J. Akerman, Appl. Phys. Lett. **92**, 092505 (2008).

[5]S. Urazhdin, P. Tabor, V. Tiberkevich, and A. Slavin, Phys. Rev. Lett. **105**, 104101 (2010).

[6]T. J. Silva, Nat. Phys. **3**, 447 (2007).

[7]R. Adler, Proc. IEEE **34**, 351 (1946).

[8]D. Li, Y. Zhou, C. Zhou, and B. Hu, Phys. Rev. B **82**, 140407(R) (2010).

[9]M. I. Rabinovich, R. Huerta, and P. Varona, Phys. Rev. Lett. **96**, 014101 (2006).

[10]S. E. Brown, G. Mozurkewich, and G. Grüner, Phys. Rev. Lett. **52**, 2277 (1984); J. Tekić, D. He, and B. Hu, Phys. Rev. E **79**, 036604 (2009).

[11]E. Stone and P. Holmes, SIAM J. Appl. Math. **50**, 726 (1990).

[12]M. W. Keller, M. R. Pufall, W. H. Rippard, and T. J. Silva, Phys. Rev. B **82**, 054416 (2010).

[13]J. Slonczewski, J. Magn. Magn. Mater. **159**, L1 (1996); L. Berger, Phys. Rev. B **54**, 9353 (1996).

[14]J. Grollier, V. Cros, and A. Fert, Phys. Rev. B **73**, 060409(R) (2006); J. Persson, Y. Zhou, and J. Akerman, J. Appl. Phys. **101**, 09A503 (2007).

[15]S. I. Kiselev, J. C. Sankey, I. N. Krivorotov, N. C. Emley, R. J. Schoelkopf, R. A. Buhrman, and D. C. Ralph, Nature (London) **425**, 380 (2003); Y. Zhou, J. Persson, S. Bonetti, and J. Akerman, Appl. Phys. Lett. **92**, 092505 (2008); J. Xiao, A. Zangwill, and M. D. Stiles, Phys. Rev. B **72**, 014446 (2005); Z. Li, Y. C. Li, and S. Zhang, *ibid.* **74**, 054417 (2006); J. Z. Sun, *ibid.* **62**, 570 (2000); G. Bertotti, C. Serpico, I. D. Mayergoyz, A. Magni, M. d'Aquino, and R. Bonin, Phys. Rev. Lett. **94**, 127206 (2005); O. Boulle, V. Cros, J. Grollier, L. G. Pereira, C. Deranlot, F. Petroff, G. Faini, J. Barnas, and A. Fert, Nat. Phys. **3**, 492 (2007); M. Gmitra, D. Horvath, M. Wawrzyniak, and J. Barnas, Phys. Status Solidi **243**, 219 (2006).

[16]C. Sperpico, R. Bonin, G. Bertotti, M. d'Aquino, and I. Mayergoyz, IEEE Trans. Magn. **45**, 3441 (2009).

[17]G. Hu, T. Ditzinger, C. Z. Ning, and H. Haken, Phys. Rev. Lett. **71**, 807 (1993); L. Gammaitoni, P. Hänggi, P. Jung, and F. Marchesoni, Rev. Mod. Phys. **70**, 223 (1998); B. Hu and C. Zhou, Phys. Rev. E **63**, 026201 (2001).

[18]T. Gilbert, IEEE Trans. Magn. **40**, 3443 (2004); X. R. Wang and Z. Z. Sun, Phys. Rev. Lett. **98**, 077201 (2007); Z. Z. Sun and X. R. Wang, Phys. Rev. B **74**, 132401 (2006).